



Measurement Of The Front Back Asymmetry In Top-Antitop Quark Pairs In 1.9 fb^{-1}

The CDF Collaboration
URL <http://www-cdf.fnal.gov>
(Dated: January 18, 2008)

A method of reconstructing $t\bar{t}$ events in the lepton plus jets mode is applied to a measurement of the forward backward asymmetry in t-tbar pair production at CDF. The measurement is a test of discrete symmetries in t-tbar production and strong interactions at large Q^2 . In the present data set it is potentially sensitive to the the presence of parity-violating production channels such as a massive Z' -like boson or new physics within Strong Interactions. Larger data sets will have sensitivity for an interesting charge asymmetry arising from pure QCD calculated at next-to-leading order. We measure the top quark forward-backward asymmetry in 1.9 fb^{-1} of CDF collision data, using 484 candidate $t\bar{t}$ lepton plus jets events in the high Pt lepton trigger streams. We measure $A_{fb} = 0.17 \pm (0.07)^{stat} \pm (0.04)^{sys}$ which can be compared to the Standard Model prediction $A_{fb} = 0.04 \pm 0.01$.

Preliminary Results for Winter 2008 Conferences

I. INTRODUCTION

Top quark physics at the Tevatron offers an interesting new forum for the study of discrete symmetries in the strong interaction: it is a strong process at very high energy. The strong interaction is currently believed to respect C,P, and T. However, there is very little test of this at high energies. As will be shown in this note, we can completely reconstruct the $t\bar{t}$ kinematics, which enables the study of charge flow on a per event basis. With the charge in hand, we can define two asymmetries:

$$A_C = \frac{N_t(p) - N_{\bar{t}}(p)}{N_t(p) + N_{\bar{t}}(p)} \quad (1)$$

$$A_{fb} = \frac{N_t(p) - N_t(\bar{p})}{N_t(p) + N_t(\bar{p})} \quad (2)$$

where $N_i(j)$ = is the number of particle i traveling in the direction of particle j

- A_C is charge symmetry; a non-zero value for this implies a net top current flowing along the proton direction.
- The front-back asymmetry, A_{fb} , is the difference in the number of top quarks flowing forward and backward along the proton direction. This kind of asymmetry is typically associated with parity-violating weak production processes. This is not expected in strong interactions, though new production mechanisms that violate parity such as a Z' particle or Top Color could appear as a front back asymmetry in top production [1] [2]. If we assume that CP symmetry is conserved then $N_{\bar{t}}(p) = N_t(\bar{p})$ and the charge asymmetry is equal to the front back asymmetry.

Although the strong interaction conserves C, QCD predicts that strong interactions produce a net charge asymmetry in the pair production of top quarks at the Tevatron. Evaluated at leading order, heavy flavor pair production via $q\bar{q}$ or gg does not discriminate between quark and anti-quark. But at next-to-leading order, radiative corrections involving a virtual or real gluon in $q\bar{q} \rightarrow Q\bar{Q}$ lead to a difference in the production of Q and \bar{Q} , and consequently a charge asymmetry. The asymmetry originates from interference between initial and final state gluon brehmsstrahlung processes, shown in Figures 1a and 1b, which produce a negative asymmetry, and the “box diagram” with the Born processes shown in Figures 1c and 1d, which produce a positive asymmetry. The overall charge asymmetry is positive and predicted to be between 4–5% by Kuhn and Rodrigo [3], and 3.8% by next-to-leading order Monte Carlo generator MC@NLO [4]. In this analysis we assume CP symmetry is conserved and therefore, the front-back asymmetry will be equal to the predicted charge asymmetry.

In this note, we present the measurement of A_{fb} in $t\bar{t}$ production, using 1.9 fb^{-1} of data. We first isolate a sample of top events and understand their backgrounds. We then develop a method to reconstruct the $t\bar{t}$ kinematics, and use it to measure the production angle of the top quark, the angle between the top quark and the proton beam. The top quark production angle is defined as:

$$\Theta = \text{Tan}^{-1} \left(\frac{P_t}{P_z} \right) \quad (3)$$

where P_z and P_t are the longitudinal and transverse momentum of the top quark in a coordinate system where the proton beam is the z-axis. The production angle distribution for the top quark, as predicted by the Monte Carlo simulation MC@NLO, is shown in Figure 2. The production angle is used to define and count the number of forward (in the proton direction) and backward (against the proton direction) events in the sample, and thus measure A_{fb} . The measured production angle is distorted from its true value by a number of experimental complications. Corrections for these effects are applied to the forward and backward counts to produce a measurement of A_{fb} which can be compared to the theoretical prediction.

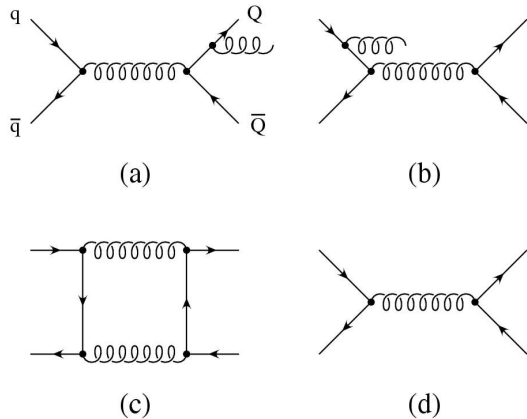
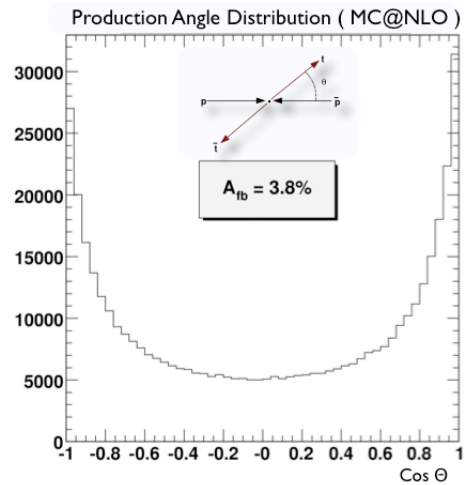


FIG. 1: NLO Diagrams

FIG. 2: $\text{Cos}(\Theta)$ Distribution MC@NLO

II. EVENT SELECTION

This analysis selects $t\bar{t}$ events in the lepton plus jets channel where one top decays semi-leptonically ($t \rightarrow l\nu b$) and the other hadronically ($t \rightarrow q\bar{q}b$). Selection begins by requiring a single high transverse momentum electron or muon in the central portion of the detector ($|p_t| > 20$ GeV/c and $|\eta| < 1.1$). In addition, we require a large amount of missing transverse energy as evidence of the presence of a neutrino ($\cancel{E}_T \geq 20$ GeV). Each event must have four or more tight jets ($|E_t| > 20$ GeV/c and $|\eta| < 2.0$) and at least one jet must have two tracks that form a secondary vertex (a "tagged" jet). A tagged jet is evidence that the jet originates from a "b" quark and therefore this requirement reduces W plus light flavor background processes which dominate the event sample. The above selection produces roughly a 5 to 1 signal to background ratio. For 1.9 fb^{-1} of data collected at CDF the number of events that pass through event selection is 484. A more complete description of the selection process can be found in the documentation of the lepton plus jets cross-section measurement [5].

III. BACKGROUNDS

Several kinds of processes without top quarks slip past our selection criteria. These events are backgrounds to the top quark signal and their presence biases and dilutes the measurement. Each background contribution for this analysis is estimated from the method described in the lepton plus jets cross-section measurement [5]. The predicted contribution for each background was calculated for an integrated luminosity of 1.9 fb^{-1} . The number of events in data that pass our selection criteria and the background estimates are shown in Tables I and II. For this analysis, we assume the number of top events is equal to the difference between data and the background estimate. The three jet bin below requires an additional loose jet ($E_t > 12$ GeV) so that this additional sample of data can be reconstructed as described in the next section.

TABLE I: Signal And Background Estimates For 1.9 fb^{-1} Pretag

Process	1 Jet	2 Jets	3.5 Jets	4 Jets	5 Jets
ww	704.6 ± 45.8	758.4 ± 49.2	59.4 ± 3.9	30.4 ± 2.0	5.6 ± 0.4
wz	103.2 ± 6.6	125.4 ± 8.0	11.0 ± 0.7	5.8 ± 0.4	1.1 ± 0.1
zz	4.7 ± 0.3	4.8 ± 0.3	0.8 ± 0.1	0.5 ± 0.0	0.1 ± 0.0
top	39.7 ± 5.3	213.3 ± 28.6	242.3 ± 32.5	403.5 ± 54.2	134.2 ± 18.0
stops	22.2 ± 2.1	51.9 ± 4.8	5.3 ± 0.5	3.3 ± 0.3	0.7 ± 0.1
stopt	63.4 ± 4.9	75.4 ± 5.8	6.2 ± 0.5	3.4 ± 0.3	0.5 ± 0.0
Z+jets	6313.9 ± 570.0	1310.1 ± 117.2	81.0 ± 7.3	34.8 ± 3.1	5.3 ± 0.5
Total HF	11292.5 ± 2504.4	3181.0 ± 705.4	277.6 ± 65.1	141.1 ± 32.3	24.8 ± 7.3
Total LF	156491.3 ± 7737.9	20182.5 ± 2324.1	1089.6 ± 200.5	430.8 ± 79.2	60.8 ± 18.9
Candidates	196007.0 ± 0.0	32194.0 ± 0.0	2302.0 ± 0.0	1223.0 ± 0.0	270.0 ± 0.0

TABLE II: Signal And Background Estimates For $1.9 fb^{-1} \geq 1$ Tag

Process	1 Jet	2 Jets	3.5 Jets	4 Jets	5 Jets
ww	12.5 ± 1.4	31.2 ± 3.5	3.6 ± 0.4	2.5 ± 0.3	0.7 ± 0.1
wz	6.9 ± 0.6	14.6 ± 1.2	1.4 ± 0.1	0.9 ± 0.1	0.2 ± 0.0
zz	0.2 ± 0.0	0.6 ± 0.0	0.1 ± 0.0	0.1 ± 0.0	0.0 ± 0.0
top	13.3 ± 1.9	107.2 ± 14.9	131.9 ± 18.3	248.1 ± 34.3	83.9 ± 11.6
stops	8.1 ± 0.8	29.9 ± 2.9	3.0 ± 0.3	2.0 ± 0.2	0.4 ± 0.0
stopt	21.4 ± 1.9	30.9 ± 2.7	3.0 ± 0.3	1.9 ± 0.2	0.3 ± 0.0
Z+jets	35.4 ± 4.6	26.4 ± 3.2	3.7 ± 0.4	2.4 ± 0.3	0.5 ± 0.1
Wbb	387.7 ± 149.2	241.0 ± 94.6	27.4 ± 11.1	16.8 ± 6.7	3.5 ± 1.5
Wcc/Wc	692.5 ± 271.2	231.7 ± 92.2	22.6 ± 9.3	13.3 ± 5.4	2.7 ± 1.2
Mistags	693.7 ± 95.7	235.6 ± 40.0	28.5 ± 6.5	16.9 ± 3.7	3.3 ± 1.1
Non-W	345.0 ± 138.0	249.4 ± 99.8	29.0 ± 11.6	13.7 ± 11.7	4.6 ± 4.6
Total	2216.6 ± 451.2	1198.6 ± 214.2	254.2 ± 30.5	318.4 ± 38.7	100.1 ± 12.9
Observed	2872.0 ± 0.0	1416.0 ± 0.0	268.0 ± 0.0	371.0 ± 0.0	113.0 ± 0.0

IV. EVENT RECONSTRUCTION

The measurement of A_{fb} will use the production angle of the top quark. The top quark is not directly observed in the detector, and therefore, we must reconstruct its momentum 4-vector from the final state particles: jets, charged leptons and neutrino. Unfortunately, we measure only the transverse component of the neutrino (in the \cancel{E}_T) and it is impossible to identify the parent quark of a jet based upon detector information. Because the type of parton cannot be identified by its jet, we cannot tell which jets came from which partons in a $t\bar{t}$ event. If we are to reconstruct the event we must find a method to choose the correct jet-parton assignments, as illustrated in Figures 3 and 4. We use an algorithm to match jets to the correct partons and reconstruct the full neutrino momentum by employing several constraints available in the “ $t\bar{t}$ lepton plus jets hypothesis”. This method allows us to reconstruct the complete kinematics of the $t\bar{t}$ final state.

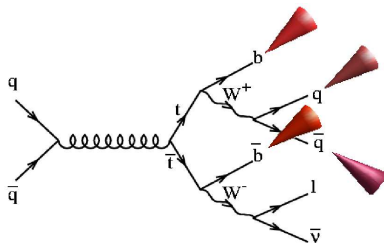
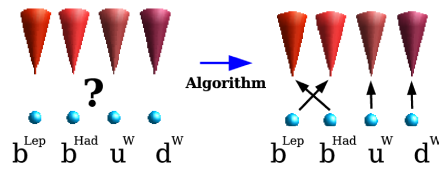
FIG. 3: $t\bar{t}$ Lepton Plus Jets Event

FIG. 4: Matching Jets To Quarks

A. Matching Jets To Quarks And Reconstructing The Neutrino

The problem of reconstructing the $t\bar{t}$ event is a combinatoric one: we must choose between a number of possible arrangements. The highest four energy jets in the event are assumed to come from the four quarks in the $t\bar{t}$ process. Matching four jets to four quarks leads to 24 possible combinations. This can be reduced by a factor of two since interchanging the two quarks from W-boson decay does not change the kinematics of the event.

Because we cannot measure the momentum of the event along the beam direction, we cannot infer the P_z of the neutrino from “missing E_z ”. However, we can calculate the neutrino P_z by requiring that the lepton and neutrino be consistent with the known mass of the W-boson. This calculation involves a quadratic equation and produces two solutions for the neutrino P_z . Both solutions are considered. Together with the jet assignments, the event has 24 possible combinations.

Our strategy is to test each combination for consistency with the “ $t\bar{t}$ hypothesis”. That hypothesis has four main components:

- The lepton and neutrino are decay products of a W-boson ($W \rightarrow l\nu$)
- Two jets are decay products of a W-boson ($W \rightarrow jj$)
- The lepton, neutrino, and a third jet are final states from a top quark decay ($t \rightarrow l\nu j$)
- The two jets from $W \rightarrow jj$ and a fourth jet are final states from the other top quark decay ($t \rightarrow jjj$)

The consistency of each combination with the $t\bar{t}$ hypothesis is assessed with a χ^2 test. The χ^2 equation is:

$$\begin{aligned} \chi^2 = & \sum_{i=l,jets} \frac{(p_t^{i,meas} - p_t^{i,fit})^2}{\sigma_i^2} + \sum_{j=x,y} \frac{(p_j^{UE,meas} - p_j^{UE,fit})^2}{\sigma_j^2} \\ & + \frac{(M_{jj} - M_W)^2}{\Gamma_W^2} + \frac{(M_{lv} - M_W)^2}{\Gamma_W^2} + \frac{(M_{bjj} - M_{fit})^2}{\Gamma_t^2} + \frac{(M_{blv} - M_{fit})^2}{\Gamma_t^2} \end{aligned} \quad (4)$$

While we are assessing the “goodness-of-fit” we can also take the opportunity to make modest corrections to the jet energies. The last four terms are the constraints. M_{jj} is the invariant mass of the two jets that must be consistent with the known W boson mass. M_{bjj} and M_{lv} are the invariant masses of the hadronically decaying and leptonically decaying top quark side. These should be consistent with being equal, and their common value, M_{fit} is the best estimate of the top quark mass. M_{lv} is the mass of the lepton and the neutrino which must be consistent with the mass of a W boson. All four of the constraints are particle masses, and their weights are the theoretical decay width of the particle.

The first two terms are sums over lepton and jet transverse energies and “unclustered” energy, which is the energy in the event outside the $t\bar{t}$ interaction. These values are varied within their measured error. This improves resolution on jet energies, as well as the probability of finding the correct combination. The known top quark mass may also be used as a further constraint in the fit by setting $M_{fit} = M_{known}$.

The standard package MINUIT is used to vary the independent parameters and minimize the χ^2 for each possible combination of jet-parton assignments and neutrino solutions [6]. The combination with the lowest χ^2 is chosen as the best representative of the $t\bar{t}$ hypothesis for the event. Tests with Monte Carlo simulations show that the correct assignment is chosen 45% of the time, and this improves to 60 % in the constrained fit. Though, incorrect combinations still provide useful information about the event kinematics.

B. The Front-Back Asymmetry

The reconstruction algorithm has been applied to $t\bar{t}$ signal and background models, and 1.9 fb^{-1} of data collected at CDF. The signal and background models are normalized to the predicted values shown in Table I . Shown in Figures 5 and 6 is the reconstructed $\text{Cos}\Theta$ and rapidity distributions for the hadronically decaying top quark where we have used the charge of the lepton, $-Q_l$, to infer the charge of the top quark. If charge conjugation symmetry is assumed in the production mechanism, then the production angle can be measured using either the hadronic or leptonic decaying top quark. The hadronic decaying top quark has been found to be more accurate in reproducing the production angle than the leptonic decaying side - mostly due to the inability to reconstruct the neutrino P_z .

The forward backward asymmetry of this distribution is calculated by:

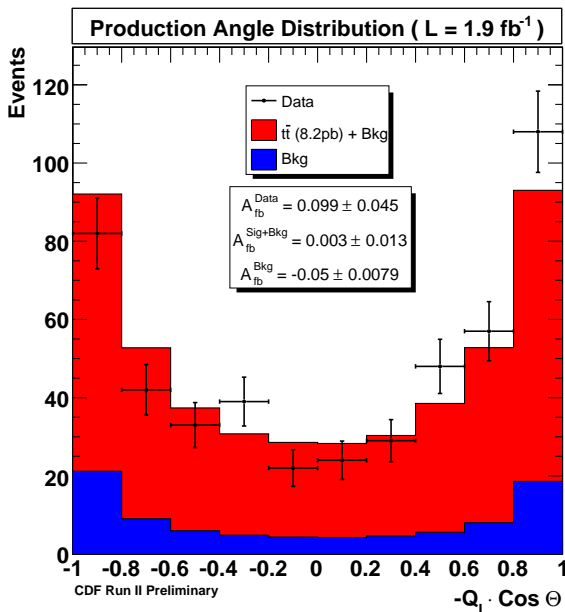
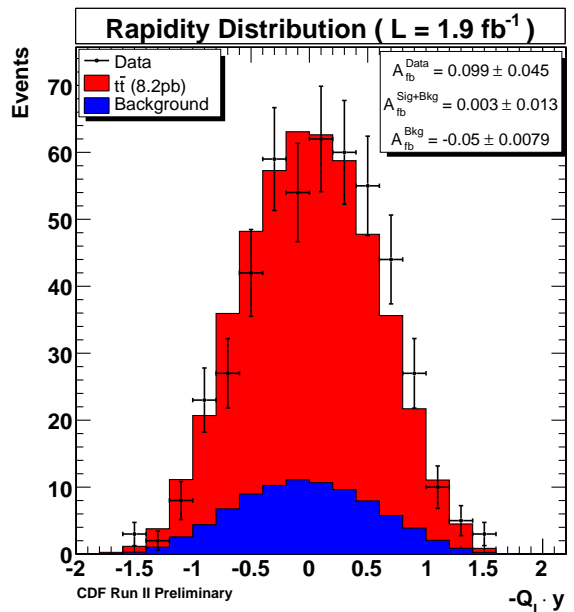
$$A_{fb} = \frac{N_{(-Q_l) \cdot \text{Cos}(\Theta) > 0} - N_{(-Q_l) \cdot \text{Cos}(\Theta) < 0}}{N_{(-Q_l) \cdot \text{Cos}(\Theta) > 0} + N_{(-Q_l) \cdot \text{Cos}(\Theta) < 0}} \quad (5)$$

The result in data and our model is:

$$A_{fb}^{data} = 0.099 \pm 0.045 \quad (6)$$

$$A_{fb}^{model} = 0.003 \pm 0.013 \quad (7)$$

The data is slightly over 2-sigma in excess from predicted. This value is skewed by backgrounds, acceptance, and reconstruction and, therefore, cannot be compared to theory. In order to make a comparison to the theoretical prediction we must understand how to correct the reconstruction back to the “true” value. The corrections to the measurement are discussed in the next section.

FIG. 5: $(-Q_l) \cdot \text{Cos}(\Theta)$ Of Hadronic Decaying TopFIG. 6: $(-Q_l) \cdot y$ Of Hadronic Decaying Top

V. CORRECTIONS TO THE MEASURED A_{fb}

In order to compare the measured front-back asymmetry to the theoretical prediction, we must account for any bias and smear of the $t\bar{t}$ asymmetry due to backgrounds, acceptance, and reconstruction. Our Monte Carlo model is expected to simulate these effects, and we use these simulations to understand and develop corrections. Each individual effect and the corresponding corrections are described in the following sections.

A. Background Corrections

All non-signal processes dilute the measurement. In addition, several of backgrounds contain intrinsic asymmetries due to parity violating weak interactions, and these will bias the measurement.

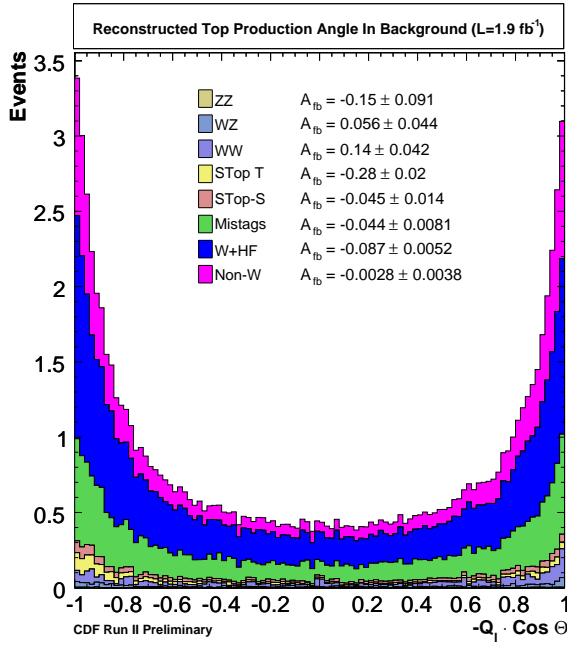
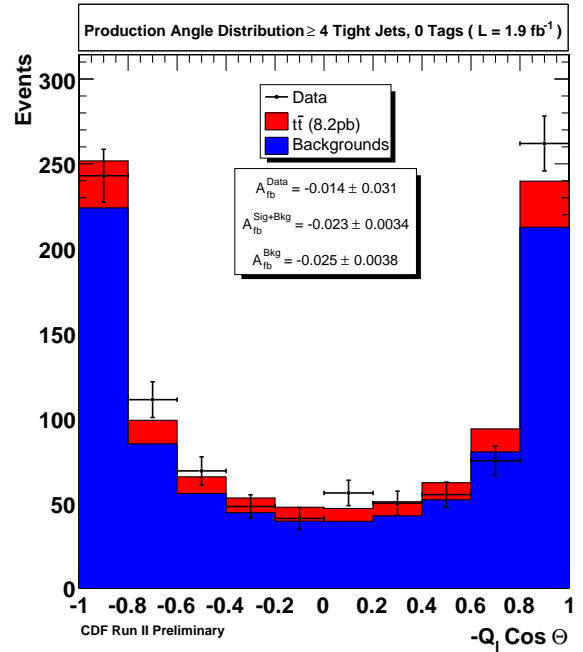
Our remediation of this complication is a straight-forward subtraction. Each background model is run through reconstruction, giving an estimate of the ratio of forward to backward events. An absolute normalization is available from the background estimate described in section III. We then subtract the predicted number of events bin by bin from the number measured in data in Figure 5.

The reconstructed production angle, $(-Q_l) \cdot \text{Cos}(\Theta)$, for the combined background model is shown in Figure 7. The contributions from the different background processes are stacked on one another. Compared to the $t\bar{t}$ signal model in Figure 5, the production angle in backgrounds is distributed much closer to the p and \bar{p} direction ($\text{Cos}(\Theta) = \pm 1$). Therefore, the signal to background ratio will be larger than average at the outer edges of this distribution.

The predicted A_{fb} and normalization for each individual background is shown within the figure. The combined background asymmetry in all lepton categories for the reconstructed production angle distribution, $(-Q_l) \cdot \text{Cos}(\Theta)$, is:

$$A_{fb}^{Total Bkg} = -0.05 \pm 0.01$$

The background has a slight asymmetry due to the presence of W +jets events. The value is negative because the W asymmetry is positive and our definition of the production angle is $(-Q_l) \cdot \text{Cos}(\Theta)$. Because the asymmetry in backgrounds is small, the largest effect the background has on the measurement is to dilute the $t\bar{t}$ signal. To test the background model we compare the $(-Q_l) \cdot \text{Cos}(\Theta)$ in a side-band to the signal region: anti-tag \geq four tight jet events. This comparison is shown in Figure 8. The shape and A_{fb} in the sideband region agree within uncertainty.

FIG. 7: $(-Q_l) \cdot \text{Cos}(\Theta)$ In BackgroundsFIG. 8: $(-Q_l) \cdot \text{Cos}(\Theta)$ Anti-Tag ≥ 4 Tight Jet Events

B. Reconstruction Corrections

Mismeasured jet energies, incorrect jet-quark assignments, and charge misidentification contribute to a smearing effect in the reconstructed production angle, which can translate into a change in the populations of events measured forward and backward. This is demonstrated in Figures 9 and 10 for Monte Carlo Top events with a +CEM electron. We see that the effect of reconstructing into the wrong hemisphere occurs for 12 to 13% of top quarks.

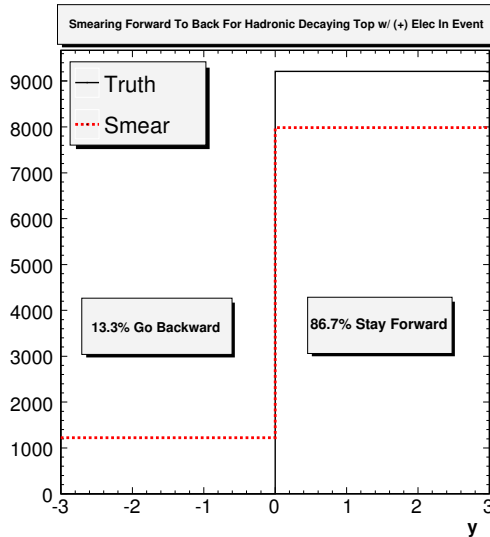


FIG. 9: Demonstration Of Forward To Backward Smearing For +CEM Electron.

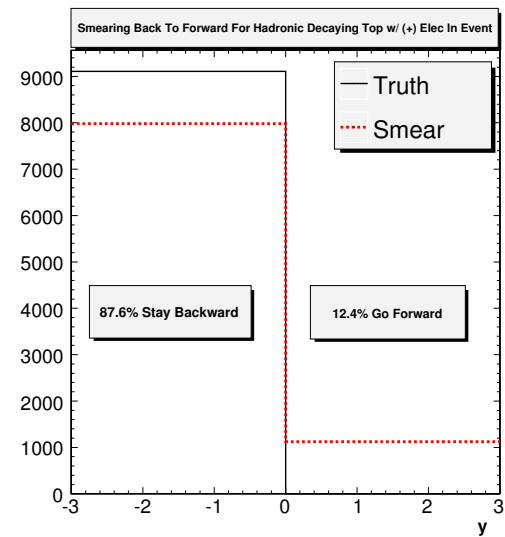


FIG. 10: Demonstration Of Backward To Forward Smearing For +CEM Electron.

With this Monte Carlo based determination of smearing, we can represent the effects of reconstruction smearing on our measurement using a matrix formalism. We define a smearing matrix as follows.

$$N_{recon} = S \cdot N_{truth-after-selection} \quad (8)$$

where,

$$S = \begin{bmatrix} S_{0,0} & S_{0,1} & \dots & \dots & S_{0,nbins} \\ S_{1,0} & S_{1,1} & \dots & \dots & \dots \\ \dots & \dots & \dots & \dots & \dots \\ S_{nbins,0} & \dots & \dots & \dots & S_{nbins,nbins} \end{bmatrix}$$

and N_{recon} and $N_{truth-after-selection}$ represent the number of events in each bin of the production angle histogram after reconstruction and after selection, respectively. The elements of the smearing matrix are defined as follows:

$$S_{i,j} = \frac{N_{recon}^{i,j}}{N_{truth}^i} \quad (9)$$

$N_{recon}^{i,j}$ = # events reconstructed in bin "j" , originally from bin "i"
 N_{truth}^i = # events in truth bin "i"

The size of the matrix is ofcourse dependent on the number of bins in the histogram. With this formalism in hand, we can invert this matrix, after background subtraction, to 'undo' the smearing effects of reconstruction. The resulting distribution represents the "true" production angle distribution after selection. We now must correct for any acceptance effects to produce a measurement that can be compared to theory.

The reconstruction matrix used in this analysis is shown below. We are using a 4x4 matrix, which produces a measurement that is invariant to any reasonable form of asymmetric production angle distribution.

$$S = \begin{bmatrix} 0.81 \pm 0.01 & 0.21 \pm 0.01 & 0.08 \pm 0.02 & 0.037 \pm 0.02 \\ 0.1 \pm 0.01 & 0.57 \pm 0.01 & 0.13 \pm 0.01 & 0.036 \pm 0.02 \\ 0.043 \pm 0.02 & 0.14 \pm 0.01 & 0.58 \pm 0.0 & 0.095 \pm 0.01 \\ 0.046 \pm 0.02 & 0.09 \pm 0.02 & 0.21 \pm 0.01 & 0.83 \pm 0.01 \end{bmatrix}$$

C. Acceptance Corrections

The reconstruction of the top quark production angle requires almost every component of the detector: hadronic and electromagnetic calorimeters, muon chambers, tracking chambers, and silicon tracking. Front-back asymmetries in detection efficiencies or acceptance will translate into an apparent asymmetry in measurement, which we will need to correct.

We use $t\bar{t}$ model to study how selection and the detector effect the measured number of events as a function of the production angle. We define the selection efficiencies as follows:

$$\epsilon_i = \frac{N_{sel}^i}{N_{gen}^i} \quad (10)$$

where,

N_{sel}^i = # events selected in MC in bin "i" of $Cos\Theta$ histogram
 N_{gen}^i = # events generated from MC in bin "i" of $Cos\Theta$ histogram

Using these efficiencies, the number of events selected for analysis can be related to those generated by matrix algebra:

$$N_{sel} = A \cdot N_{gen} \quad (11)$$

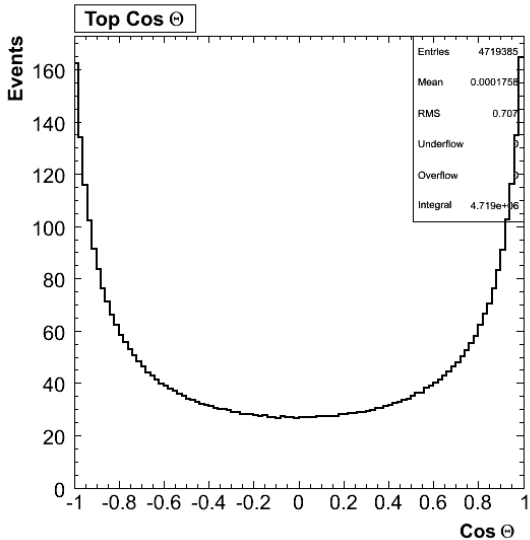


FIG. 11: Production Angle Before Cuts

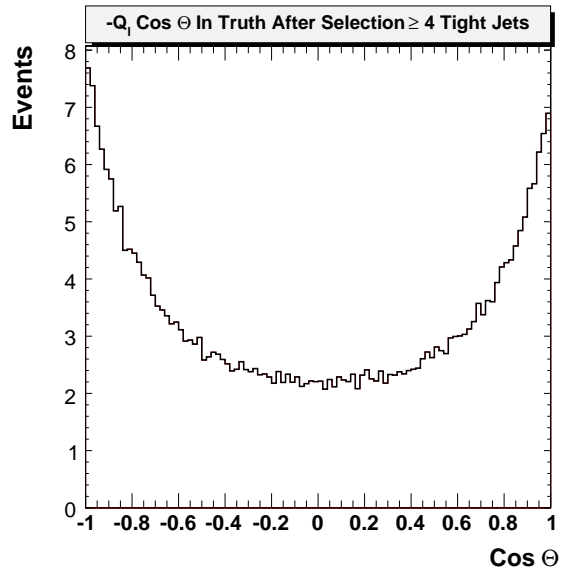


FIG. 12: Production Angle After Cuts

where,

$$A = \begin{bmatrix} \epsilon_0 & 0 & \dots & 0 & 0 \\ 0 & \epsilon_1 & 0 & 0 & 0 \\ \dots & 0 & \dots & 0 & 0 \\ 0 & 0 & \dots & \epsilon_{nbins-1} & 0 \\ 0 & 0 & \dots & 0 & \epsilon_{nbins} \end{bmatrix}$$

and N_{sel} , N_{gen} are just column matrices representing the number of events in each bin of a histogram. The acceptance matrix used in this analysis is shown below.

$$A = \begin{bmatrix} 0.97 \pm 0.01 & 0 & 0 & 0 \\ 0 & 1.20 \pm 0.01 & 0 & 0 \\ 0 & 0 & 1.10 \pm 0.01 & 0 \\ 0 & 0 & 0 & 0.90 \pm 0.01 \end{bmatrix}$$

A simple visualization of the efficiency matrix is to just divide the production angle distribution at the HEPG level after selection by that before selection. These two histograms are shown in Figures 12 and 11. The resulting acceptance plot is shown in Figure 13. Notice the asymmetric acceptance as a function of the production angle. This can be understood by looking at the production angle distribution after selection for 4 tight jet events and ≥ 5 tight jet events separately, which are shown in Figures 15 and 16. Notice that the asymmetry appears almost entirely in the 5 jet bin. Figure 14 is a breakdown of Figure 16 into top and anti-top but without multiplying by charge. Clearly a charge asymmetry exists in the Monte Carlo. Initial state radiation contributes far more to the 5 jet bin than the 4 jet bin. $t\bar{t}$ events at the Tevatron usually produce top on-shell. Therefore, the top quark is more connected to the incoming quark in the proton and the anti-top is more connected to the incoming anti-quark in the anti-proton. When the top is produced in the direction of the proton, the angle between the incoming quark and the top is small. Color flow dictates that any radiation is limited to this small angle. Conversely, when the top quark is angled in the opposite direction, the radiation can emit from a much larger angle. Therefore, it is more likely to pick up 5 tight jet events in the case that top is traveling in the opposite direction of the incoming proton the vice-versa. This produces a charge asymmetry, as seen in Figure 12.

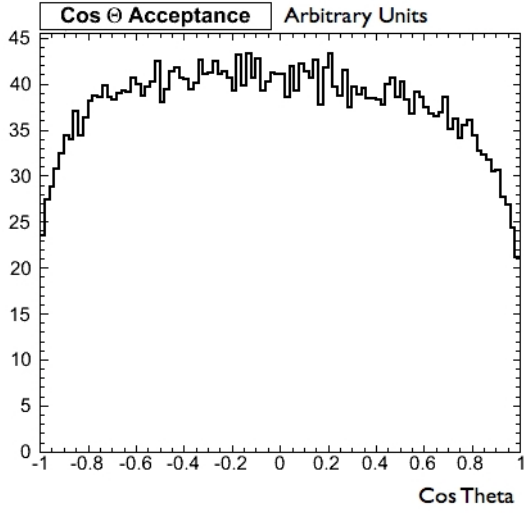


FIG. 13: Acceptance as a function of production angle ≥ 4 Tight Jets

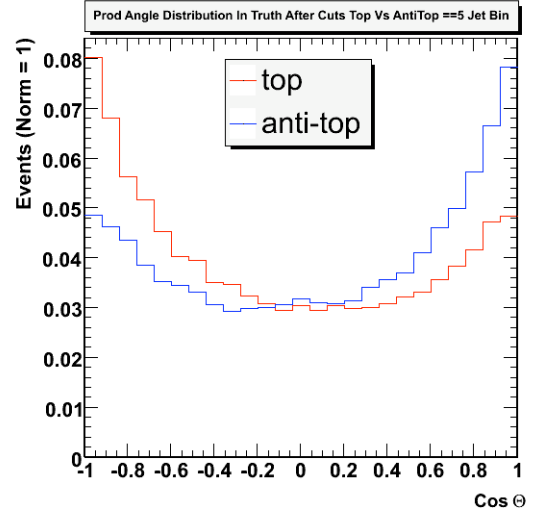


FIG. 14: Production Angle After Cuts ≥ 5 Jets (top and anti-top)

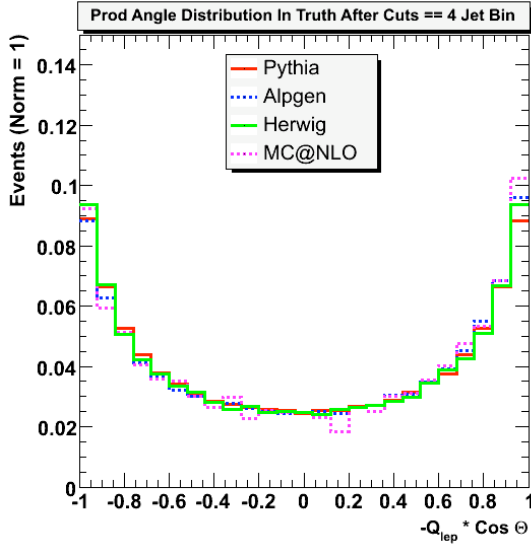


FIG. 15: Production Angle After Cuts = 4 Jets

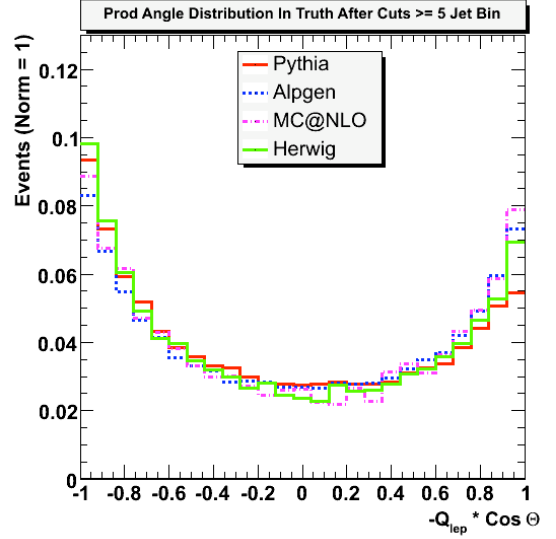


FIG. 16: Production Angle After Cuts ≥ 5 Jets

D. Total Correction To The Measured A_{fb}

With the understanding of acceptance and reconstruction bias in hand, we can develop an overall formalism for correcting the measured A_{fb} back to the true A_{fb} of $t\bar{t}$ production. Matrices A and S are multiplied together to create a relationship between the background corrected number of forward and backward events and the true number of forward and backward events generated in Monte Carlo. We will call the corrected values that are comparable to the number of events generated $N_{corrected}$.

$$N_{bkg-sub} = S \cdot A \cdot N_{truth} \quad (12)$$

The combined matrix formed by multiplication of A and S is then inverted so that we can solve for the corrected values.

$$N_{corrected} = A^{-1} \cdot S^{-1} \cdot N_{bkg-sub} \quad (13)$$

This technique is used to calculate the final corrected asymmetry that may be compared to theoretical prediction. The forward backward asymmetry is calculated as follows. Let,

$$\alpha = [1, 1, \dots, 1, 1] \quad (14)$$

$$\zeta = [1, 1, \dots, 1, -1, \dots, -1, -1] \quad (15)$$

Then

$$A_{fb} = \frac{\zeta \cdot N_{corrected}}{\alpha \cdot N_{corrected}} \quad (16)$$

The uncertainty on this equation is slightly more complicated. To simplify some algebra let:

$$N = N_{corr} \quad (17)$$

$$n = N_{bkg-sub} \quad (18)$$

$$M = A^{-1} \cdot S^{-1} \quad (19)$$

So,

$$N = M \cdot n \quad (20)$$

is equivalent to equation 13. A_{fb} can then be represented as a sum:

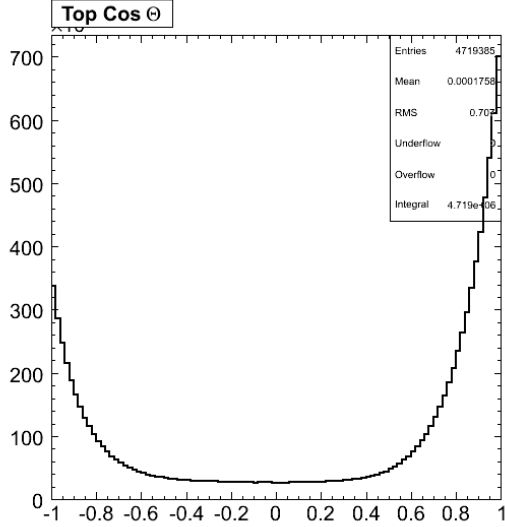
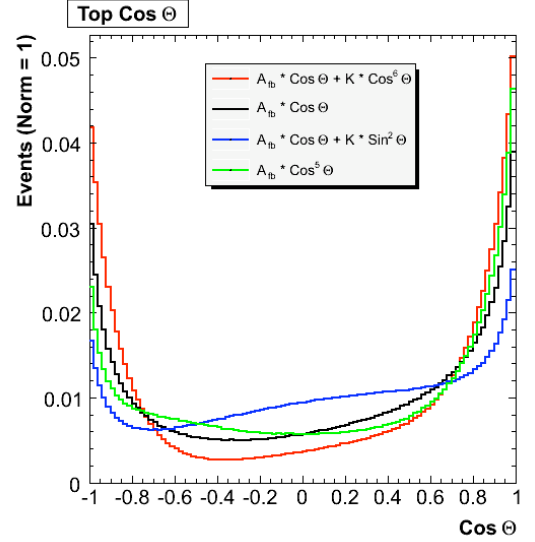
$$A_{fb} = \frac{\sum_i \zeta_i \sum_j^{nbins} M_{i,j} \cdot n_j}{\sum_i \alpha_i \sum_j^{nbins} M_{i,j} \cdot n_j} \quad (21)$$

Now we just perform simple error propagation:

$$\sigma_{A_{fb}}^2 = \sum_i \sigma_{n_i}^2 \cdot \left(\frac{\delta A_{fb}}{\delta n_i} \right)^2 \quad (22)$$

where, σ_{n_i} = the statistical uncertainty in bin "i" for background corrected data and,

$$\frac{\delta A_{fb}}{\delta n_x} = \frac{(\sum_i \zeta_i \cdot M_{i,x}) \cdot (\alpha \cdot N) - (\sum_i \alpha_i \cdot M_{i,x}) \cdot (\zeta \cdot N)}{(\alpha \cdot N)^2} \quad (23)$$

FIG. 17: Exotic Production Angle Distribution $A_{fb} = 0.3$ FIG. 18: Exotic Production Angle Distributions $A_{fb} = 0.2$

E. Underlying Distribution Effects

The "true" underlying distribution, that is the production angle distribution from nature that is producing our measurement may have drastically different shape than anticipated by the Monte Carlo. Because we use a matrix inversion technique, a simple form of unfolding, the measurement is somewhat invariant to this shape. The higher the binning or size of matrix the more measurement is invariant to this effect. To study this, we reweight our $t\bar{t}$ Monte Carlo to produce a more exotic production angle shape. This is shown in Figure 17. The symmetric term in this distribution is reweighted to add a 6th order term in $\text{Cos}\Theta$ in order to produce a shape with far more events out on the edges. Events near the edges are less likely to cross the forward-backward boundary and therefore less smearing occurs than distributions that have a bulk of the events near this boundary. The acceptance and reconstruction matrices are made from Monte Carlo with zero asymmetry and a symmetric distribution predicted by the Standard Model. If the "true" distribution has more events on the edges than predicted by our model, then it is easy to imagine we are over-correcting - predicting more smearing than actually occurs. We can test this by putting the exotic distribution in Figure 17 through the machinery of this analysis. The result is shown in Table III. As expected the 2x2 matrix over-corrects the distribution by about 17%. Surprisingly, simply moving to a 4x4 matrix drastically reduces this over-correction, as does a 10x10. Because of this, as mentioned earlier, we will use a 4x4 matrix as opposed to a 2x2. Ultimately, the best thing to do is use as large a matrix as possible, but this leads to bin to bin oscillation effects in matrix inversion that only regularized unfolding techniques can solve. Regularized unfolding is more advanced than really required for this analysis, therefore we will stay with 4x4.

TABLE III: A_{fb}^{True} Vs $A_{fb}^{Measured}$ Exotic Distribution Test

A_{fb}^{True}	2x2	4x4	10x10
0.3	0.35 ± 0.01	0.31 ± 0.01	0.31 ± 0.01

This test can be expanded to study how the 4x4 matrix corrects several different kinds of underlying distributions. Figure 18 shows various production angle distributions, all with $A_{fb} = 0.2$. If our matrix correction technique is robust, then it should be able to handle the differences between these distributions and return the true $A_{fb} = 0.2$. Each distribution is put through the entire framework of our analysis: selection, reconstruction, and corrections. The result of this test, shown in Table 18, is that the 4x4 matrix correction technique is robust against a wide range of underlying distributions.

TABLE IV: A_{fb}^{True} Vs $A_{fb}^{Measured}$ Further Exotic Distribution Tests

Distribution	A_{fb}^{True}	$A_{fb}^{corrected}$
$A_{fb} \cdot \text{Cos}\Theta + K \cdot \text{Cos}^6\Theta$	0.2	0.22 ± 0.01
$A_{fb} \cdot \text{Cos}\Theta$	0.2	0.21 ± 0.01
$A_{fb} \cdot \text{Cos}\Theta + K \cdot \text{Sin}^2\Theta$	0.2	0.22 ± 0.01
$A_{fb} \cdot \text{Cos}^5\Theta$	0.2	0.20 ± 0.01

VI. SYSTEMATIC UNCERTAINTIES

A number of systematic effects contribute to our measurement uncertainty in a way that is not yet reflected in our calculation. Each systematic is estimated in a unique way, but the general procedure is to compare the measured result of a $t\bar{t}$ Monte Carlo model with $A_{fb} = 0.2$ before and after a systematic has been varied. The Jet Energy Scale is estimated by fluctuating the model by the known uncertainties in JES by $\pm 1\sigma$. Samples of Monte Carlo were generated with more and less initial and final state radiation to estimate the impact of each. As described above, this measurement has been tested for a number of different underlying production angle distributions. The variance between different distributions has been taken as a systematic. The normalization of our background and the shape of the Monte Carlo model are varied within error and the difference in the measurement of our example models is taken as a systematic. Finally, we use 46 different sets of PDF and compare to the default set used. Table V summarizes the uncertainty taken for each systematic effect. The dominant uncertainty is due to background shape and normalizations, and top mass - though the top mass systematic is most likely due to limited statistics in that comparison. The combined systematic uncertainty on the measurement of A_{fb} is calculated by adding each individual uncertainty in quadrature. The result is:

$$\sigma_{syst} = \pm 0.04 \quad (24)$$

TABLE V: Systematic Uncertainties

Systematic	$-\Delta$	$+\Delta$	σ
MC Gen	0.0	0.012	0.012
JES	-0.005	0.004	0.005
ISR	0.0	0.004	0.004
FSR	-0.013	-0.007	0.012
Top Shape	-0.012	0.008	0.012
Bkg Shape	-0.008	0.018	0.018
Bkg Norm	-0.014	0.021	0.021
PDF	-0.011	0.011	0.011
Total			0.038

VII. MEASUREMENT

We now carry out the full method described in this note to measure the forward-backward asymmetry for 1.9 fb^{-1} of data collected at CDF. Candidate $t\bar{t}$ lepton plus jets events are selected in data and the top production angle for each event is reconstructed. The number of events in four equal sized bins (two forward and two backward) are counted, and the predicted background contributions in these bins are subtracted. Bias and smearing are corrected with the procedure described in section V. The front-back asymmetry is calculated from the corrected forward and backward counts by:

$$A_{fb} = \frac{N_{Forward} - N_{Backward}}{N_{Forward} + N_{Backward}} \quad (25)$$

The step-by-step details of this procedure for 1.9 fb^{-1} of data collected at CDF are now described.

A. Event Selection and Reconstruction

The 484 candidate events are selection as described in section II. These events are reconstructed using the kinematic fitter in a constrained fit. The production angle distribution of the hadronically decaying top quark, $-Q_l \cdot \text{Cos}(\Theta)$, is produced. This is shown in Figure 19. The raw asymmetry in data is:

$$A_{fb}^{data} = 0.099 \pm 0.045 \quad (26)$$

B. Background Corrections

We rebin the reconstructed distribution into four equal size bins and get the bin contents for background and data. The result is shown in Table VI and the rebinned histogram is shown in Figure 20.

TABLE VI: Bin Contents in data and background

	bin 0	bin 1	bin 2	bin 3
data	141	77	72	194
background	33.4	12.0	11.5	29.6
bkg-corrected	107.6	65.0	60.5	164.4

The background corrected asymmetry is:

$$A_{fb}^{bkg-sub} = 0.13 \pm 0.06 \quad (27)$$

C. Reconstruction and Acceptance Corrections

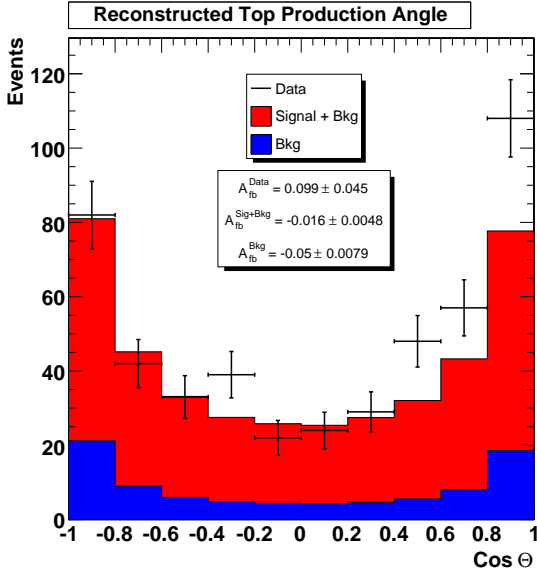
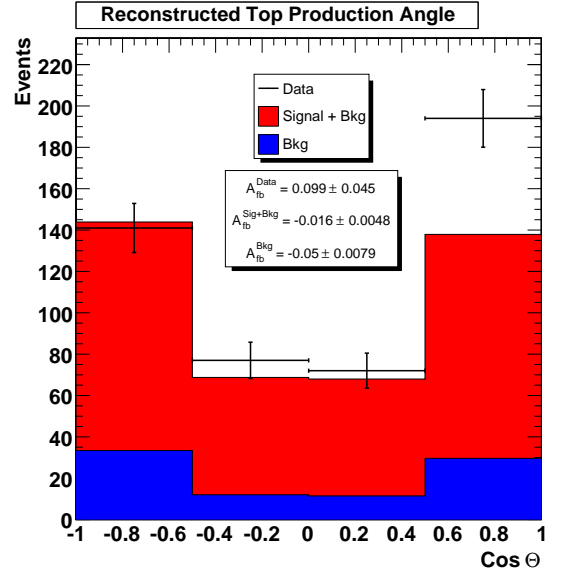
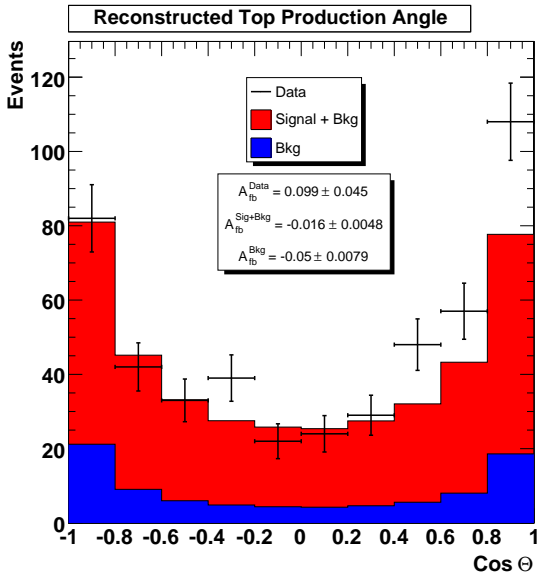
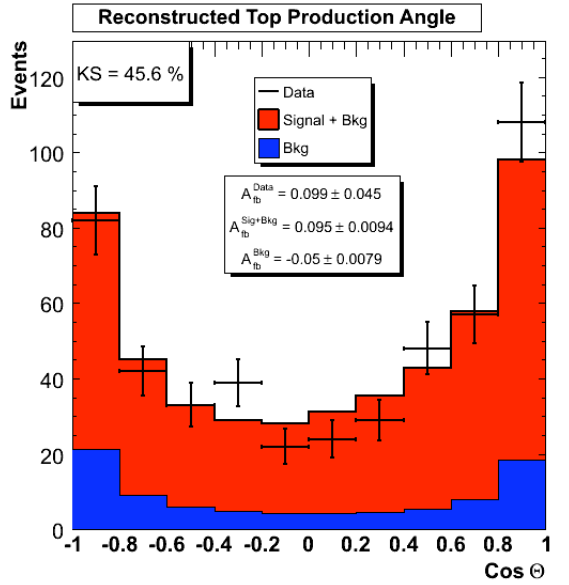
We now recast the background corrected data from Table VI as a single column matrix (n) and apply the acceptance and reconstruction matrices.

$$N_{corrected} = A^{-1} \cdot S^{-1} \cdot n$$

$$N_{corrected} = \begin{bmatrix} 0.97 & 0 & 0 & 0 \\ 0 & 1.20 & 0 & 0 \\ 0 & 0 & 1.10 & 0 \\ 0 & 0 & 0 & 0.90 \end{bmatrix}^{-1} \cdot \begin{bmatrix} 0.81 & 0.21 & 0.08 & 0.037 \\ 0.1 & 0.57 & 0.13 & 0.036 \\ 0.043 & 0.14 & 0.58 & 0.095 \\ 0.046 & 0.09 & 0.21 & 0.83 \end{bmatrix}^{-1} \cdot \begin{bmatrix} 107.6 \\ 65.0 \\ 60.5 \\ 164.4 \end{bmatrix}$$

Propagating the background subtracted data through our correction matrices and calculating the front back asymmetry we measure:

$$A_{fb}^{measured} = 0.17 \pm (0.07)_{stat} + (0.04)_{sys} \quad (28)$$

FIG. 19: $(-Q_l) \cdot \text{Cos}(\Theta)$ Of Hadronic Decaying TopFIG. 20: $(-Q_l) \cdot \text{Cos}(\Theta)$ Of Hadronic Decaying Top - RebinnedFIG. 21: $(-Q_l) \cdot \text{Cos}(\Theta)$ Of Hadronic Decaying TopFIG. 22: $(-Q_l) \cdot \text{Cos}(\Theta)$ Of Hadronic Decaying Top - Reweighted signal $A_{fb} = 0.17$

D. Template Check

We can perform a cross-check to the measurement by reweighting a Monte Carlo $t\bar{t}$ distribution to have a "true" $A_{fb} = 0.17$ and check that the raw asymmetries after reconstruction agree. The raw distribution in data along with the predicted model (before reweighting) are shown in Figure 21. We reweight the $t\bar{t}$ signal model and normalize the signal to the data to compare the reconstructed asymmetries. This is shown in Figure 22. For a "true" $A_{fb} = 0.17$ the reconstructed asymmetry is predicted to be $A_{fb} = 0.095 \pm 0.01$. This is in very good agreement with the raw value in data: $A_{fb} = 0.099 \pm 0.045$. A KS test is performed to compare the shape of the reweighted distribution with backgrounds and data. The result, $\text{KS} = 45.6\%$ is also in good agreement.

VIII. CONCLUSION

We have developed a method of reconstructing $t\bar{t}$ events in the lepton plus jets mode and applied this to a measurement of the front-back asymmetry in top production in 1.9 pb^{-1} of proton-antiproton collisions at $\sqrt{s} = 1.96 \text{ TeV}$. The measurement is a test of charge asymmetry in the strong interaction at large momentum transfer. In the present data set it is also potentially sensitive to large parity violating contributions to top production. The front-back asymmetry is measured to be:

$$A_{fb} = 0.17 \pm (0.07)^{stat} \pm (0.04)^{syst}$$

The measured asymmetry is consistent (at the 2σ level) with the theoretical prediction 0.04.

Acknowledgments

We thank the Fermilab staff and the technical staffs of the participating institutions for their vital contributions. This work was supported by the U.S. Department of Energy and National Science Foundation; the Italian Istituto Nazionale di Fisica Nucleare; the Ministry of Education, Culture, Sports, Science and Technology of Japan; the Natural Sciences and Engineering Research Council of Canada; the National Science Council of the Republic of China; the Swiss National Science Foundation; the A.P. Sloan Foundation; the Bundesministerium für Bildung und Forschung, Germany; the Korean Science and Engineering Foundation and the Korean Research Foundation; the Science and Technology Facilities Council and the Royal Society, UK; the Institut National de Physique Nucleaire et Physique des Particules/CNRS; the Russian Foundation for Basic Research; the Comisión Interministerial de Ciencia y Tecnología, Spain; the European Community's Human Potential Programme; the Slovak R&D Agency; and the Academy of Finland.

-
- [1] M.Carena, A.Daleo, B.A.Dobrescu, T.Tait, "Z' Gauge Bosons At The Tevatron", hep-ph/0408098 (2004).
 - [2] C.T. Hill, "Topcolor Assisted Technicolor", Phys. Lett. B 345, 483 (1995).
 - [3] J.H. Kuhn and G. Rodrigo, Phys. Rev. Lett. 81, 49 (1998)
J.H. Kuhn and G. Rodrigo, Phys. Rev. D 59, 054017(1999).
 - [4] S. Frixione and B.R. Webber, "Matching NLO QCD computations and parton shower simulations", JHEP 0206 (2002) 029 [hep-ph/0204244]
S. Frixione, P. Nason and B.R. Webber, "Matching NLO QCD and parton showers in heavy flavour production", JHEP 0308 (2003) 007 [hep-ph/0305252]
 - [5] CDF Collaboration, "Measurement of the $t\bar{t}$ Production Cross Section in $p\bar{p}$ collisions at $\sqrt{s} = 196$ TeV using Lepton + Jets Events with Secondary Vertex b-tagging", CDF Note 8795
http://www-cdf.fnal.gov/physics/new/top/confNotes/cdf8795_SecVtxXSPublic.ps
 - [6] F.James, "MINUIT: Function Minimization and Error Analysis Reference Manual", <http://wwwasdoc.web.cern.ch/wwwasdoc/minuit/minmain.html>, Computing And Networks Division, CERN (1998).